EUROPEAN JOURNAL OF PHYCOLOGY, 2020
https://doi.org/10.1080/09670262.2020.1750059

Morphological and molecular characterization of *Heterocapsa claromecoensis* sp. nov. (Peridiniales, Dinophyceae) from Buenos Aires coastal waters (Argentina)

Inés Sunesen [a], Francisco Rodríguez [b], Jonás A. Tardivo Kubis[a], Delfina Aguiar Juárez[a], Antonella Risso[a], Andrea S. Lavigne[a], Stephan Wietkamp [c], Urban Tillmann [c] and Eugenia A. Sar [a]

[a]División Ficología Dr. Sebastián Guarrera, FCNyM, UNLP, Paseo del Bosque s/n, 1900, La Plata, Argentina; [b]Instituto Español de Oceanografía, Subida a Radio Faro 50-52, 36390 Cabo Estay, Vigo, Spain; [c]Alfred Wegener Institut, Helmholz-Zentrum für Polar- und Meeresforschung, Am Handelshafen 12, D – 27570, Bremerhaven, Germany

ABSTRACT

A new species of the marine dinophyte genus *Heterocapsa* Stein is described. Two clonal strains originating from Argentinean coastal waters were examined with light and electron microscopy and LSU and ITS rDNA sequence data were obtained. *Heterocapsa claromecoensis* sp. nov. is described as a distinctive species with a conical epitheca, a similar sized and rounded hypotheca, a single reticulate chloroplast situated in the periphery of the cell, and a large pyrenoid in the episome, above an ellipsoidal to rounded nucleus in the hyposome. The plate tabulation pattern of Po (pore plate), cp (cover plate), X (X-plate or canal plate), 5', 3a, 7'', 6c, 5s, 5''', 2'''' was as for most other species of *Heterocapsa*. *H. claromecoensis* sp. nov. differs from all other species of *Heterocapsa* by the microarchitecture of two different types of organic body scales, which uniquely were different in height. Phylogenetic trees based on LSU and ITS rDNA sequences placed *H. claromecoensis* in a separate branch, with a sequence assigned to *H. orientalis* being the closest match based on LSU rDNA.

ARTICLE HISTORY Received 17 December 2019; revised 9 March 2020; accepted 25 March 2020

KEYWORDS Body scales morphology; cell morphology; Dinophyceae; *Heterocapsa*; *Heterocapsa claromecoensis*; molecular characterization; phylogeny

Introduction

Heterocapsa is an important marine, thecate, photosynthetic dinoflagellate genus including very widely distributed and bloom-forming species, two of which (*H. circularisquama* Horiguchi and *H. bohaiensis* J.Xiao & Y.Li) were identified as causing harmful effects (Horiguchi, 1995; Xiao *et al.*, 2018).

Heterocapsa was described by Stein (1883) and later emended by Iwataki & Fukuyo in Iwataki *et al.* (2003) to include 3-D triradiate body scales as an important generic criterion. The taxonomic history of *Heterocapsa* was comprehensively summarized by Iwataki (2008), but he was not aware that the nomenclatural status of *Heterocapsa* is challengeable. As pointed out in a recent series of papers (Tillmann *et al.*, 2017a; Gottschling *et al.*, 2018a, b, 2019), a nomenclatural pitfall has been recognized only recently. Briefly, when Stein (1883) founded the genus *Heterocapsa* he formally based the type species *H. triquetra* on the basionym *Glenodinium triquetrum* Ehrenberg. However, consulting and analysing Ehrenberg's original material in the Ehrenberg Collection located at the 'Herbarium am Museum für Naturkunde' in Berlin revealed that Stein obviously did not inspect Ehrenberg's original drawings, which definitely identify *Glenodinium triquetrum* as a species of *Kryptoperidinium* (Gottschling *et al.*, 2018a, 2019). To avoid unwarranted nomenclatural changes (i.e. *Heterocapsa* would have to be used for species today assigned to *Kryptoperidinium*, and all species currently assigned to *Heterocapsa* would have to be transferred to *Cachonina*), and because *Heterocapsa triquetra* sensu Stein has had no validly published name, Tillmann *et al.* (2017a) described *Heterocapsa steinii* Tillmann, Gottschling, Hoppenrath, Kusber & Elbrächter typified with Stein's original illustration and epitypified it with material from the type locality. In a second step, to keep the taxonomic concept of *Heterocapsa sensu* Stein, it was then proposed to conserve the name *Heterocapsa* with *H. steinii* as conserved type (Gottschling *et al.*, 2018b). As a formal decision of the General Committee on this proposal is pending, we follow the existing usage of *Heterocapsa* according to the Rec. 14 A of the ICN for algae, fungi and plants (Turland *et al.*, 2018) for this paper.

Currently, the most important generic diagnostic morphological character of *Heterocapsa* is the presence of 3-D delicate body scales on the cell surface. The thecal plate pattern (Po, cp, X, 4–5', 2–3a, 6–7'',

CONTACT Urban Tillmann urban.tillmann@awi.de; Eugenia A. Sar easar@fcnym.unlp.edu.ar

Published online 23 Jul 2020

6c, 5s, 5‴, 2⁗) is of a peridinioid type and slightly variable: whereas most species have five apical, three anterior intercalary and seven precingular plates, the type species *H. steinii* (= *H. triquetra sensu* Stein) has four apical, two anterior intercalary and six precingular plates (Lindemann, 1924; Balech, 1988; Tillmann *et al.*, 2017a). For all *Heterocapsa* species the large anterior sulcal plate (as) is located ventrally in the precingular series, reaching almost the middle of the epitheca (Iwataki *et al.*, 2002a, 2003; Iwataki, 2008). Almost all 17 currently accepted species in this genus are well described with respect to detailed morphology of the cells and of the body scales (Iwataki *et al.*, 2004; Salas *et al.*, 2014). The combination of characters useful for identification of species are based on cell shape, size and proportions of epitheca/hypotheca, size and relative location of the nucleus and pyrenoid, and ultrastructure of the pyrenoid and of the body scales (Horiguchi, 1995; Iwataki *et al.*, 2002a, b, 2003, 2004, 2009; Tamura *et al.*, 2005; Iwataki, 2008).

The aim of this paper was to describe a new species of *Heterocapsa* based on the detailed study of cell morphology, thecal tabulation, body scale ultrastructure and phylogenetic analyses of the LSU and ITS rDNA sequences, and to compare it with morphologically and phylogenetically allied species.

Materials and methods

Isolation and culture of strains

Clonal strains of *Heterocapsa* were established from surface water samples collected with 30 µm net hauls from Claromecó, Province of Buenos Aires, Argentina (Fig. 1), on 24/10/2016. Single cells were isolated by micropipette under an Axiovert 40 CFL microscope with phase contrast and DIC (Zeiss Microimaging, Goettingen, Germany). Individual cells were washed several times in local filtered seawater and, when free of contaminants, they were transferred into 6-well tissue culture plates containing 10 ml natural seawater enriched with Guillard's f/2 medium (Sigma Aldrich, Saint Louis, Missouri, USA). Cells were incubated at 16°C, 12:12 light:dark cycle, under light supplied by cool-white fluorescent tubes, in a controlled environment growth chamber (SEMEDIC I-290F, SEMEDIC SRL, CABA, Argentina). After successful isolation, cultures were scaled up to 40 ml in Erlenmeyer flasks and incubated in the conditions described. One of the successfully scaled up strains was labelled LPCc-005 and was identified as representing a new species of the genus *Heterocapsa*.

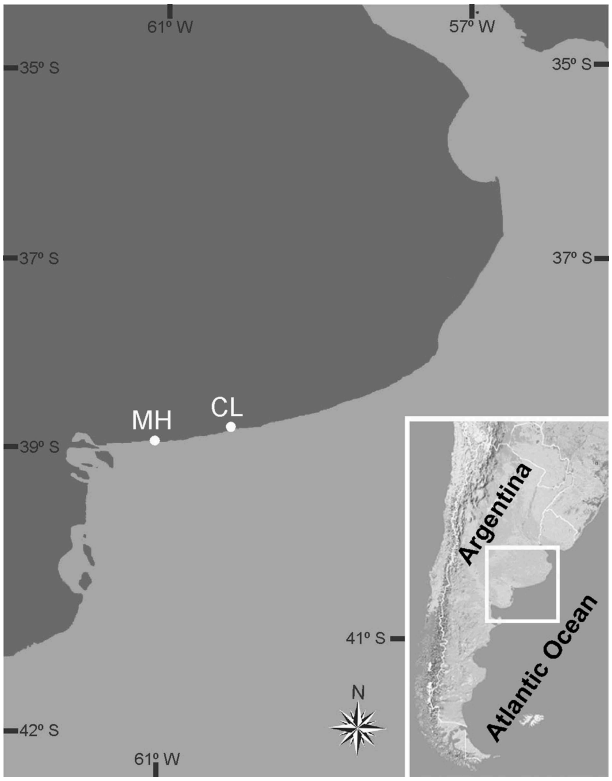

Fig. 1. Map of the Province of Buenos Aires showing sampling stations and location of the study area in Argentina. CL: Claromecó, MH: Monte Hermoso.

This strain was morphologically and genetically compared with another strain isolated from Monte Hermoso, Province of Buenos Aires, Argentina. This clonal strain (Arg-B5) was established by single cell isolation in June 2015 from a bottle sample (1.5 m depth) taken from a sandy beach surf zone (temp: ~14°C, salinity ~35) in late May 2015. The strain was routinely grown at 15° C and 50 µmol photons m^{-2} s^{-1} using a North Sea water based (salinity 33) K-medium (Keller *et al.*, 1987).

Microscopy

Light microscopy

Cells of strain LPCc-005 were observed alive or fixed with formaldehyde, 4% final concentration, using an Axiovert 40 CFL (Zeiss) inverted microscope and a Leica DMLA microscope (Leica Microsystems, Wetzlar, Germany) equipped with DIC and UV epifluorescence optics. For analyses of the cell thecal plate arrangement, specimens were stained with calcofluor white (Fluorescent Brightener 28, Sigma Aldrich) following Fritz & Triemer (1985). Cells were also dissected, with the aid of distilled water, leaving them to dry on the slides and squashing them gently by pressing on the coverslip. Cells of strain Arg-B5 were observed using an inverted microscope (Axioskop 200M, Zeiss) and a compound

microscope (Axioskop 2, Zeiss), both equipped with epi-fluorescence and differential interference contrast optics. Photographs of both strains were taken with a digital camera (AxioCam HRc, Zeiss).

Scanning electron microscopy

Cells of strain LPCc-005 were fixed with formaldehyde (4% final concentration) and kept at room temperature for 1–30 days. One ml of the suspension was collected on nylon (polyamide) filter membranes (13 mm diameter, 0.45 µm pore-size, Sartolon polyamide, Sartorius Stedim Biotech GmbH, Goettingen, Germany) in a filter funnel, rinsed several times in filtered seawater with distilled water in increasing proportions (Arbeláez *et al.*, 2017), and then dehydrated in a series of 30%, 50%, 70%, 90%, 95% and 100% of ethanol (EtOH) for 10 min each. Filters were critical-point-dried (model CPD-30, BalTec, Balzers, Liechtenstein), and mounted on aluminium stubs. Samples were either sputter-coated with gold with a JFC 1100 FC (JEOL, Tokyo, Japan) and subsequently observed with a JSM 6360 LV (JEOL) or with gold palladium with a Cressington 108 (Cressington Scientific Instruments, Watford, UK) and a NTS SUPRA 40 FE-SEM (Zeiss). Cells of strain Arg-B5 were collected, prepared and viewed as described by Tillmann *et al.* (2019).

Transmission electron microscopy

Cells (strain LPCc-005) from growing cultures were initially fixed with 2% glutaraldehyde made up with 0.2 M phosphate buffer pH 7.4, at 4°C for 2 hours. Cells were rinsed with the phosphate buffer, postfixed with 1% osmium tetroxide diluted in distilled water at 4°C for 2 hours, dehydrated in a series of 30%, 50%, 75%, 95% and 100% ethanol (24 hours each) and finally in 100% acetone (24 hours). Subsequently, the samples were embedded with Araldite resin (Huntsman Advanced Materials Inc., Basel, Switzerland) and polymerized at 60°C, for 24 hours, under soft vacuum. Ultrathin sections of 60 nm thickness were cut on a Leica EM UC7 ultramicrotome (Leica). Sections were collected onto a copper grid and contrasted with 1% uranyl acetate and lead citrate. Thin sections were observed under a JEM 1200 – EX II (JEOL). Digitized images were taken with an Erlangshen ES 1000W (Gatan, Pleasanton, California, USA).

DNA extraction and PCR amplification

Molecular analyses of strain LPCc-005 were performed on single cells, which were picked manually with a glass micropipette, washed in two drops of milli-Q water and placed in 200 µl microtubes. They were frozen in liquid nitrogen and samples kept at −20°C until further processing. DNA extraction used a modified Chelex procedure (Richlen & Barber, 2005). Briefly, 100 µl of 10% Chelex100 (Bio-Rad, Hercules, California, USA) in milli-Q water was added and samples were transferred to 200 µl tubes. The samples were heated to 95°C in a Mastercycler EP5345 (Eppendorf AG, Hamburg, Germany) for 10 min, then vortexed. The heating and vortex steps were done twice. Samples were centrifuged (13000 rpm, 2 min) and the supernatants were transferred to clean 200 µl microtubes avoiding the Chelex beads and stored at −20°C until further processing. The domain D1–D3 of the LSU rDNA and both internal transcribed spacers (ITS1 and ITS2) including the 5.8S rDNA region were amplified in Surecycler 8800 thermal cycler (Agilent Technologies, Santa Clara, USA) using the pairs of primers D1R/LSUB (5'-ACCCGCTGAATTTAAGCATA-3'/5'-ACGAA CGATTTGCACGTCAG-3'; Lenaers *et al.*, 1989; Litaker *et al.*, 2003) and ITSF01/PERK-ITS-AS (5'-GAGGAAGGAGAAGTCGTAACAAGG-3'/5'-GC TTACTTATATGCTTAAATTCAG-3'; Kotob *et al.*, 1999; Ki & Han, 2007). PCR conditions for LSU rDNA amplification followed Rodríguez *et al.* (2017). For ITS rDNA, PCR conditions were as follows: 4 min initial denaturing at 94°C, followed by 30 cycles of 30 s denaturing at 94°C, 1 min annealing at 55°C, and 2 min elongation at 72°C, with a final elongation step of 10 min at 72°C. For strain Arg-B5, DNA extraction and PCR amplification were performed as described in Tillmann *et al.* (2017b).

The PCR products of strain LPCc-005 were purified with ExoSAP–IT (USB, Cleveland, Ohio, USA), and PCR products of strain Arg-B5 were purified using the NucleoSpin Gel and PCR clean-up kit (Macherey-Nagel, Düren, Germany). All purified PCR products were sequenced using the Big Dye Terminator v.3.1 reaction cycle sequencing kit (Applied Biosystems, Foster City, California, USA). LPCc-005 PCR sequences were obtained on an ABI Prism 3130 Genetic Analyzer (Applied Biosystems) at the CACTI sequencing facilities (Universidad de Vigo, Spain), and Arg-B5 sequences were generated on an ABI 3730xl DNA Sequencer (Applied Biosystems) by the Eurofins sequencing facilities (Eurofins Genomics, Ebersberg, Germany).

The ITS region (660 nt (LPCc-005) and 656 nt (Arg-B5)), and D1–D3 region of LSU rDNA (889 nt (LPCc-005) and 699 nt (Arg-B5)) sequences obtained

in this study were deposited in GenBank (accession numbers shown in Figs 48 and 49 and in the molecular diagnosis).

Phylogenetic analyses

Sequences were inspected and aligned using MEGA 7 (Kumar *et al.*, 2016). LSU and ITS rDNA alignments included 696 and 585 final positions, respectively. Phylogenetic model selection employed MEGA 7. A Tamura–Nei (TN93+G, gamma shape parameter $\gamma = 0.27$) model was selected for LSU, while Kimura 2-parameter (K2+G, $\gamma = 0.28$) was selected for ITS phylogeny. Sequences from the genera *Karlodinium, Takayama* and *Scrippsiella* were used to root the LSU and ITS trees. Phylogenetic relationships were also determined using Bayesian inference and in this case the substitution models were obtained by sampling across the entire GTR model space following the procedure described in the manual for MrBayes v3.2. Bayesian trees were constructed with MrBayes v3.2 (Huelsenbeck & Ronquist, 2001) and the program parameters were statefreqpr = dirichlet (1,1,1,1), nst = mixed, rates = gamma. The phylogenetic analyses involved two parallel analyses, each with four chains. Starting trees for each chain were selected randomly using the default values for MrBayes. The corresponding number of unique site patterns for LSU and ITS rDNA alignments were 197 and 272, respectively. One million generations were used in these analyses. Posterior probabilities were calculated from every 100th tree sampled after log-likelihood stabilization ("burn-in" phase). Maximum likelihood (ML) phylogenetic analyses were conducted in MEGA 7. Bootstrap values were estimated from 1000 replicates. Overall topologies resulting from ML and Bayesian inference (BI) methods were very similar. The ML phylogenetic trees are shown with bootstrap values and posterior probabilities from BI. Uncorrected *p*-distances (proportion (*p*) of nucleotide sites at which two sequences are different (Transitions + Transversions)) were calculated using MEGA 7. Thus, no corrections for multiple substitutions at the same site, substitution rate biases (e.g. differences in the transitional and transversional rates), or differences in evolutionary rates among sites are considered (Nei & Kumar, 2000).

Results

Morphological analyses

Heterocapsa claromecoensis Sunesen, Rodríguez, Tillmann & Sar, _sp. nov._ (Figs 2–47)

Description: Cells 16–30 µm long and 12–25 µm wide. Epitheca somewhat conical, hypotheca rounded, similar in size. Cingulum excavated, wide, descending. Sulcus slightly depressed. A single chloroplast situated in the periphery of the cell. A large pyrenoid, with tubular cytoplasmic invaginations, in the episome above an ellipsoidal to rounded nucleus in the hyposome. Plate tabulation pattern Po, cp, X, 5', 3a, 7'', 6c, 5s, 5''', 2''''. Two types of complex 3-D body scales on the cell surface, flat and high scales, both types with six ridges from the centre of the basal plate, nine peripheral uprights, one central spine, three intermediate bars which radiate from the central spine and furcate into two lateral and one central bar, three upper bars radiating from distal part of the central spine, and 12 peripheral bars (six shorter and six longer), connecting nine peripheral uprights. Each lateral bar was connected with the corresponding longer peripheral bar by a small bar. Length of the central spine much greater in the high scales (> 200 nm) than in the flat ones (< 100 nm), angle between the central spine and descending bars acute in the high scales and almost straight in the flat ones.

HOLOTYPE: Formaldehyde-fixed material of strain LPCc-005 was deposited in the Herbarium of the División Ficología 'Dr. Sebastián A. Guarrera', under the sample number LPC 11462 here designated, labelled 'holotype of *Heterocapsa claromecoensis*, prepared from strain LPCc-005, Claromecó, 24/10/2016'.

ISOTYPE: Formaldehyde-fixed material of strain LPCc-005 was deposited in the Herbarium of the División Ficología 'Dr. Sebastián A. Guarrera', under the sample number LPC 11462 here designated, labelled 'isotype of *Heterocapsa claromecoensis*, prepared from strain LPCc-005, Claromecó, 24/10/2016'.

TYPE LOCALITY: Claromecó (38°51'29" S–60°01'28" W), Province of Buenos Aires, Argentina.

STRAIN ESTABLISHMENT: Authentic strain LPCc-005, established from material sampled on 24/10/2016 and isolated on 25/10/2016 by I. Sunesen, available from División Ficología, FCNyM, UNLP, Argentina. Strain Arg-B5 established from a sample collected in Monte Hermoso on 27/5/2015 by V. Guinder and isolated on 2/6/2015 by U. Tillmann (this strain is lost and no longer available).

MOLECULAR DIAGNOSIS: Strain LPCc-005, LSU (MK684238) and ITS rDNA (MK684239); strain Arg-B5, LSU (MN509451) and ITS rDNA (MN509452).

HABITAT: Marine coastal waters, plankton.

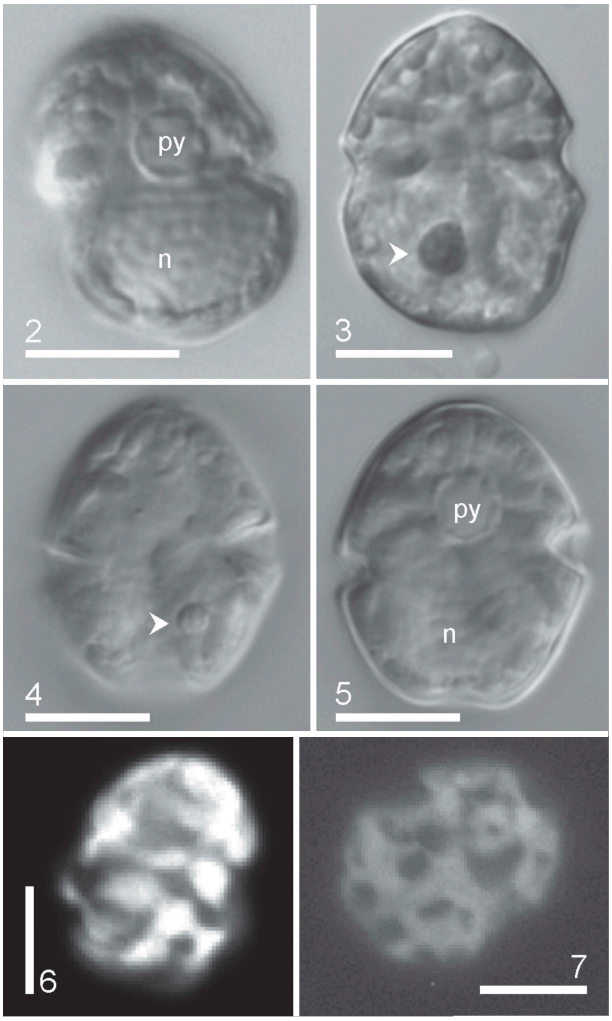

Figs 2–7. *Heterocapsa claromecoensis* sp. nov. LM. **Figs 2, 3, 6, 7**. Strain LPCc-005; **Figs 4, 5**. Strain Arg-B5. **Figs 2–5**. Live cells or Lugol's preserved cells observed in brightfield. Figs 2, 5. Note one pyrenoid (py) in the episomes and a large, ellipsoidal nucleus (n) in the hyposomes. Figs 3, 4. Note the small red accumulation body (arrowhead). **Figs 6, 7**. Cells observed with epifluorescence. Note the reticulate chloroplasts. Scale bars = 10 μm (Figs 2–7).

ETYMOLOGY: The specific epithet is derived from Claromecó, which is the name of the beach from where the species was collected.

Detailed description

Cells were small, ovoid, and had a delicate theca. Cells of strain LPCc-005 were 16–30 μm in length (n = 80) and 12–25 μm in width (n = 80), and strain Arg-B5 20–28 in length (n = 50) and 16–24 μm in width (n = 50). The epitheca was somewhat conical, similar in size to slightly smaller than the rounded hypotheca (Figs 2–5). The cingulum was excavated, wide, and slightly descending, displaced by almost ½ of its own width (Figs 11, 13). The sulcus was slightly depressed and sometimes did not reach the posterior end of the hypotheca (Fig. 13). The single chloroplast was reticulate in structure and parietal in position (Figs 6, 7), and there was a large pyrenoid located in the episome above the nucleus, which was surrounded by a starch sheath (Figs 2, 5, 34–37). The nucleus, with condensed chromosomes visible with LM, was large, ellipsoidal and positioned in the hyposome, occupying most of it (Figs 2, 5, 34, 35). Some cells had a red accumulation body in the hyposome (Figs 3, 4). Cell division was by oblique binary fission in the motile stage (not shown). Thecal plates were thin and observable with LM after dissection, but were only revealed well by fluorescence microscopy and scanning electron microscopy (Figs 8–19). The basic thecal plate pattern was Po, cp, X, 5', 3a, 7", 6c, 5s, 5"', 2"" (Figs 38–41). Exceptional deviations from this common pattern in the precingular series (with six instead of seven plates) and postcingular series (with five instead of six plates) were observed in strain LPCc-005. The apical pore complex (APC) was composed by a pore plate (Po), sub-hexagonal in outline. In the centre of the pore plate there was a pore surrounded by a roundish rim (Fig. 18). The pore was occluded by a cover plate (cp) accompanied by a hinge structure (Fig. 18). Five apical plates (Figs 11, 15, 18) and a small sub-circular canal plate (X) surrounded Po (Figs 8, 18, 40). The X plate was displaced to the cell's right side, placed somewhat asymmetrically between the two larger apical plates, 1' and 5' (Figs 8, 18, 40). The dorsal apical plate 3' was shorter than plate 4' or both plates were similar in size in some specimens (Figs 10, 12, 14, 15, 39, 40). There were three anterior intercalary plates in dorsal position (Figs 12, 14, 15, 40). Plate 2a was the largest of the intercalary plates, with 2a and 3a being hexagonal in outline, whereas plate 1a was pentagonal (Figs 12, 14, 15, 40). Plate 3a was characteristic in shape and position and was located parallel next to the plate 4' (Figs 10, 14, 15). Precingular plates were commonly seven (Figs 9, 10, 15, 38–40). The row of precingular plates was interrupted by the large anterior sulcal plate (as), which was irregularly pentagonal and placed between the pentagonal plate 1" and the trapezoidal plate 7" (Figs 8, 9, 11, 13, 17, 38). The plates 2" to 6" were adjacent to the anterior intercalary plates (Figs 8–10, 15, 17, 40). There were five postcingular plates (Figs 16, 44). Plates 1"' and 5"' were rectangular to trapezoidal (Figs 8, 9, 11, 13, 38, 41), and 2"' to 4"' were trapezoidal to pentagonal (Figs 12, 14, 16, 39). The hypotheca was

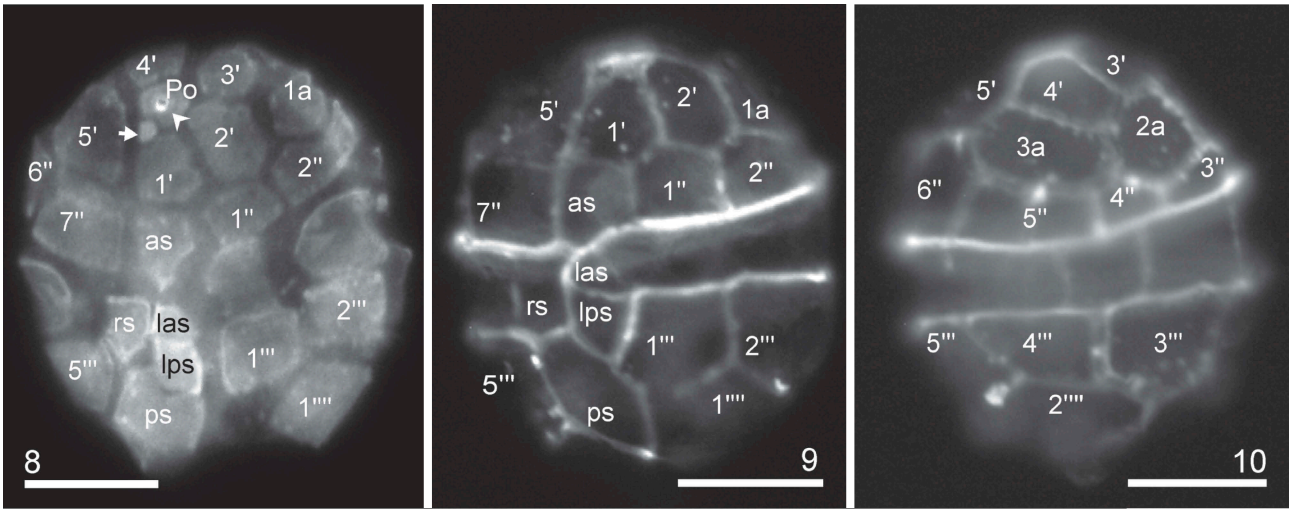

Figs 8–10. *Heterocapsa claromecoensis* sp. nov. LM images of strain LPCc-005 with UV excitation after calcofluor staining to illustrate plate arrangement. **Fig. 8**. Cell in ventral view. Note a pore plate (Po), the pore (arrowhead), the sub-circular X plate (arrow). **Figs 9, 10**. Same cell in two focal planes. Fig. 9. Focus on the ventral side. Fig. 10. Focus on the dorsal side (note that this view is mirror-imaged). Plate labels according to the Kofoidian system. Labels of sulcal plates, as: anterior sulcal, las: left accessory sulcal, lps: left posterior sulcal, rs: right sulcal, ps: posterior sulcal. Scale bars = 10 μm (Figs 8–10).

completed by two antapical plates that were pentagonal and similar or slightly dissimilar in size (Figs 12–14, 16, 41). Cingular plates were six. In the sulcal region, plate c1 abutted on the left anterior sulcal plate (las), and plate c6 abutted on the right sulcal plate (rs) (Figs 19, 38). The sulcal area was composed by five plates, including an anterior sulcal plate (as), a hemispherical left anterior sulcal plate (las), and a subrectangular left posterior sulcal plate (lps) (Figs 8, 9, 19, 38). The right sulcal plate (rs) was irregularly hexagonal, and bordered plates as, las, lps, ps, 7", 5''' and c6 (Figs 19, 38). The posterior sulcal plate (ps) with a distal tongue-shaped end abutted with plates rs and lps (Figs 8, 9, 19, 38) and 1''', 5''', 1'''' and 2'''' (Figs 13, 16, 19, 38). Numerous trichocyst pores were present on the thecal plates with a more or less scattered pattern (Figs 11–14, 16–19). On precingular and postcingular plates some of the pores were arranged in rows on the margin towards the cingulum, and on cingular plates towards both margins (Figs 19, 20). On the apical plates pores were randomly scattered (Fig. 18). There were many pores on the pore plate whereas the X plate consistently was free of pores (Fig. 18). The cell surface was covered by two different types of complex body scales placed on the external cell membrane (Figs 20–33, 42–47). Flat scales were < 100 nm in height, much more triangular in outline and slightly small in diameter, whereas high scales were > 200 nm in height, subtriangular and more rounded in outline and slightly larger in diameter (Figs 22–33, 42–47). Both scale types had the same geometric organization and were composed by a basal plate which was 250–420 nm in diameter with six radial ridges (Figs 25, 26, 29–33). SEM micrographs were not able to resolve details of the basal plate texture, but Figs 25, 28 and 32 indicate that the basal plate was fine and not coarsely reticulate. One central spine and nine peripheral uprights, three on each corner (Figs 22–33, 42–47), arose from the basal plate. The radial ridges of the basal plate radiated from the central spine to the base of the six external peripheral uprights, two for each triplet (Figs 25, 31, 42–47). Three intermediate bars radiated from the central spine (Figs 25–33, 42, 43). Each intermediate bar was divided into three, the two lateral bars were slightly descending and joined to the external uprights of two contiguous groups of three uprights; the central of the three formed bars was upward and supported two long peripheral bars (Figs 25, 26, 29, 31, 33, 42, 43). Peripheral uprights were connected by peripheral bars (six shorter and six longer) (Figs 22–33, 45–47). Each lateral bar was connected to the corresponding longer peripheral bar by a small bar parallel to the central bar (Figs 25, 27, 28, 42 '8'). Completing the structure, three upper bars radiated from the distal part of the central spine and joined to the longer peripheral bars (Figs 44–47). These descending bars had a diameter similar to the central spine. The much greater length of the central spine in the high scales

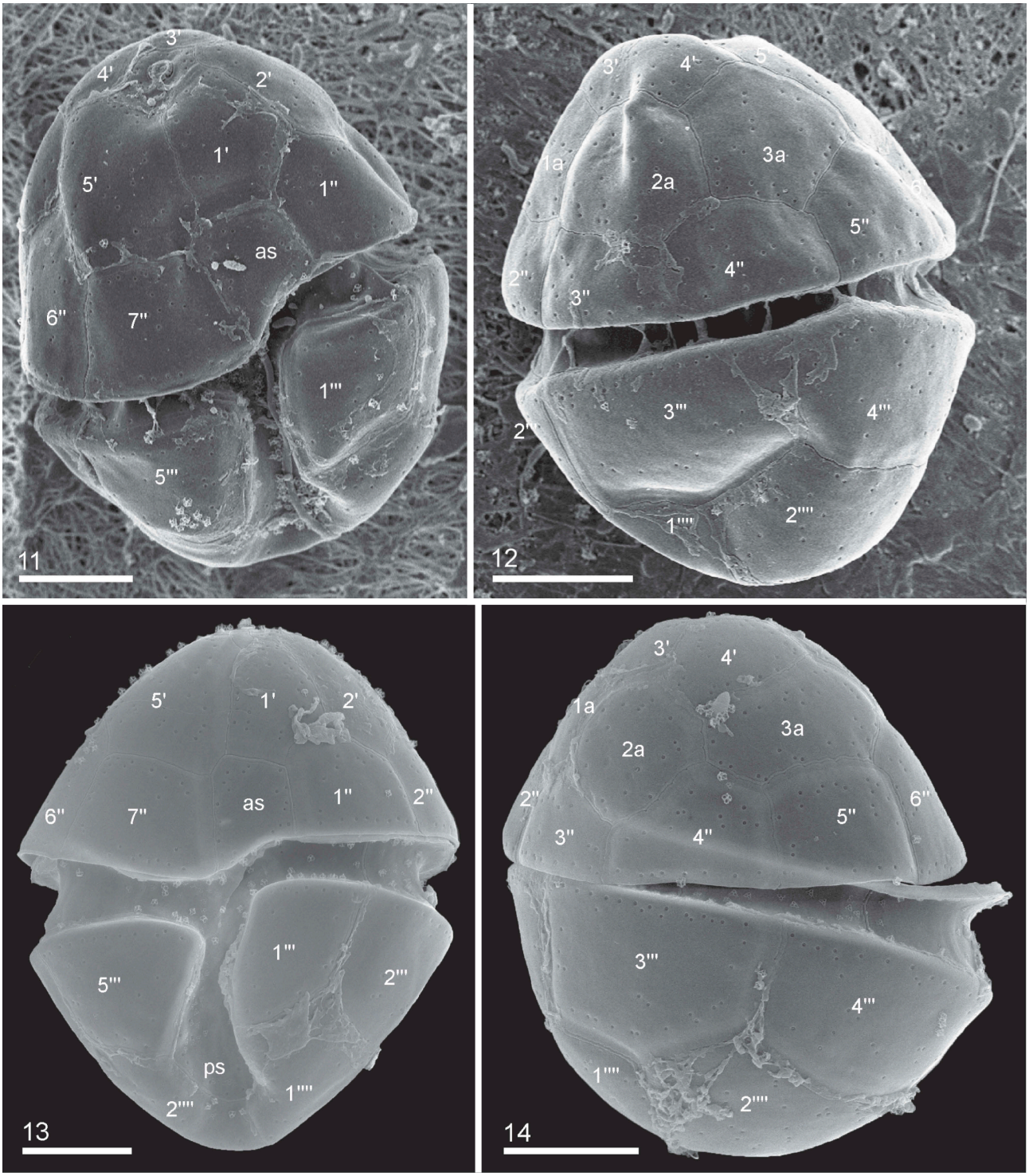

Figs 11–14. *Heterocapsa claromecoensis* sp. nov. **Figs 11, 12**. SEM images of strain LPCc-005. Fig. 11. Cell in ventral view. Fig. 12. Cell in dorsal view. **Figs 13, 14**. SEM images of strain Arg-B5. Fig. 13. Cell in ventral view. Fig. 14. Cell in dorsal view. Plate labels according to the Kofoidian system. Scale bars = 5 μm (Figs 11–14).

compared with the flat ones means that the angle formed between the central spine and the descending bars was acute in the high scales and almost a right-angle in the flat ones (Figs 25–27, 30–32, 42–47).

Transmission electron microscopy revealed the dinokaryon with condensed chromosomes (Figs 34–36) and a conspicuous nucleolus (Fig. 34). The spherical pyrenoid was connected to the chloroplast and was surrounded by a starch sheath (Figs 34, 35). The pyrenoid

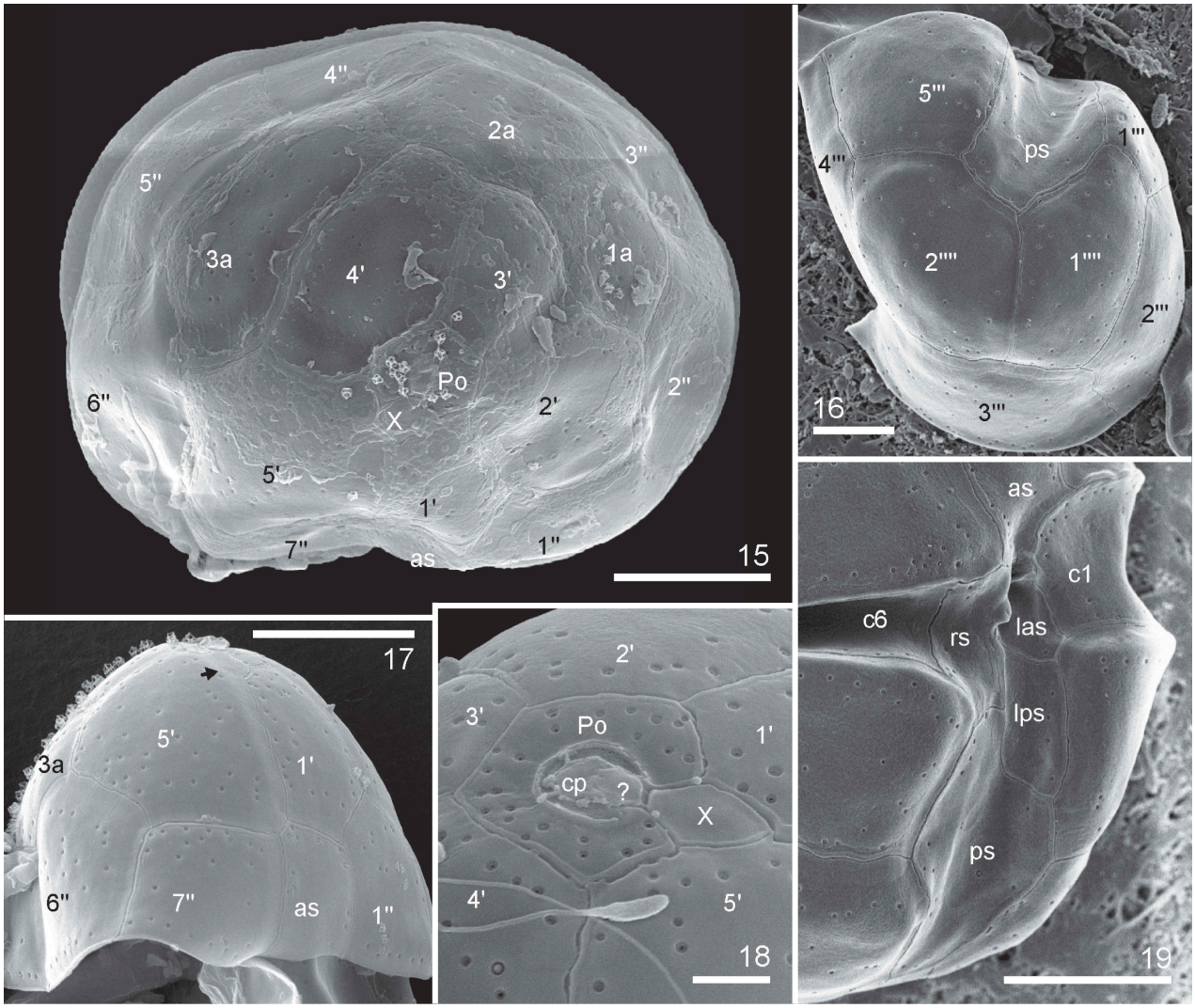

Figs 15–19. *Heterocapsa claromecoensis* sp. nov. SEM. Figs 15, 17, 18. Strain Arg-B5. Figs 16, 19. Strain LPCc-005. **Fig. 15**. Cell in apical view showing the plate pore (Po), the X plate, five apical plates, three intercalary plates and seven precingular plates. **Fig. 16**. Hypotheca in antapical view showing two antapical plates, slightly different in size, five postcingular plates and the posterior sulcal plate. **Fig. 17**. Epitheca in lateral ventral view with two larger plates 5' and 6'' limiting with the 3a. Note the presence of some body scales. Arrow shows the X plate. **Fig. 18**. Detail of epitheca in apical view showing the Po, the cover plate (cp) occluding the pore, the hinge structure (marked as ?), the X plate, and the five apical plates. **Fig. 19**. Detail of the sulcal area showing sulcal plates (as, las, lps, rs, ps) and two cingular plates (c1 and c6). Plate labels according to the Kofoidian system. Scale bars = 5 μm (Figs 15–17, 19), 1 μm (Fig. 18).

was crossed by many tubular invaginations but without penetration of thylakoid lamellae (Figs 36, 37).

Molecular analyses

LSU and ITS rDNA based phylogenies (Figs 48, 49) placed the sequences of *Heterocapsa claromecoensis* LPCc-005 and Arg-B5 in distinct branches relative to other genetic clades including identified and unidentified strains of *Heterocapsa*. The overall topology was somewhat different in LSU and ITS phylogenies, as a consequence of the different species and strains available for each region.

LSU phylogeny (Fig. 48) showed *H. orientalis* Iwataki, Botes & Fukuyo as the closest species to *H. claromecoensis*. The two *H. claromecoensis* LSU rDNA sequences were identical but of different length (889 nt for LPCc-005; 699 nt for Arg-B5). *Heterocapsa orientalis* was only available for LSU, for 515 nt length. When aligned these three sequences just shared a common fragment of 341 nt given that the Arg-B5 sequence was for LSU positions 61–760, LPCc-005 was 69–958, and *H. orientalis* was 418–933. Considering the short common fragment for all three sequences, LSU sequences of *H. claromecoensis* and *H. orientalis* were similar and displayed only four mismatches

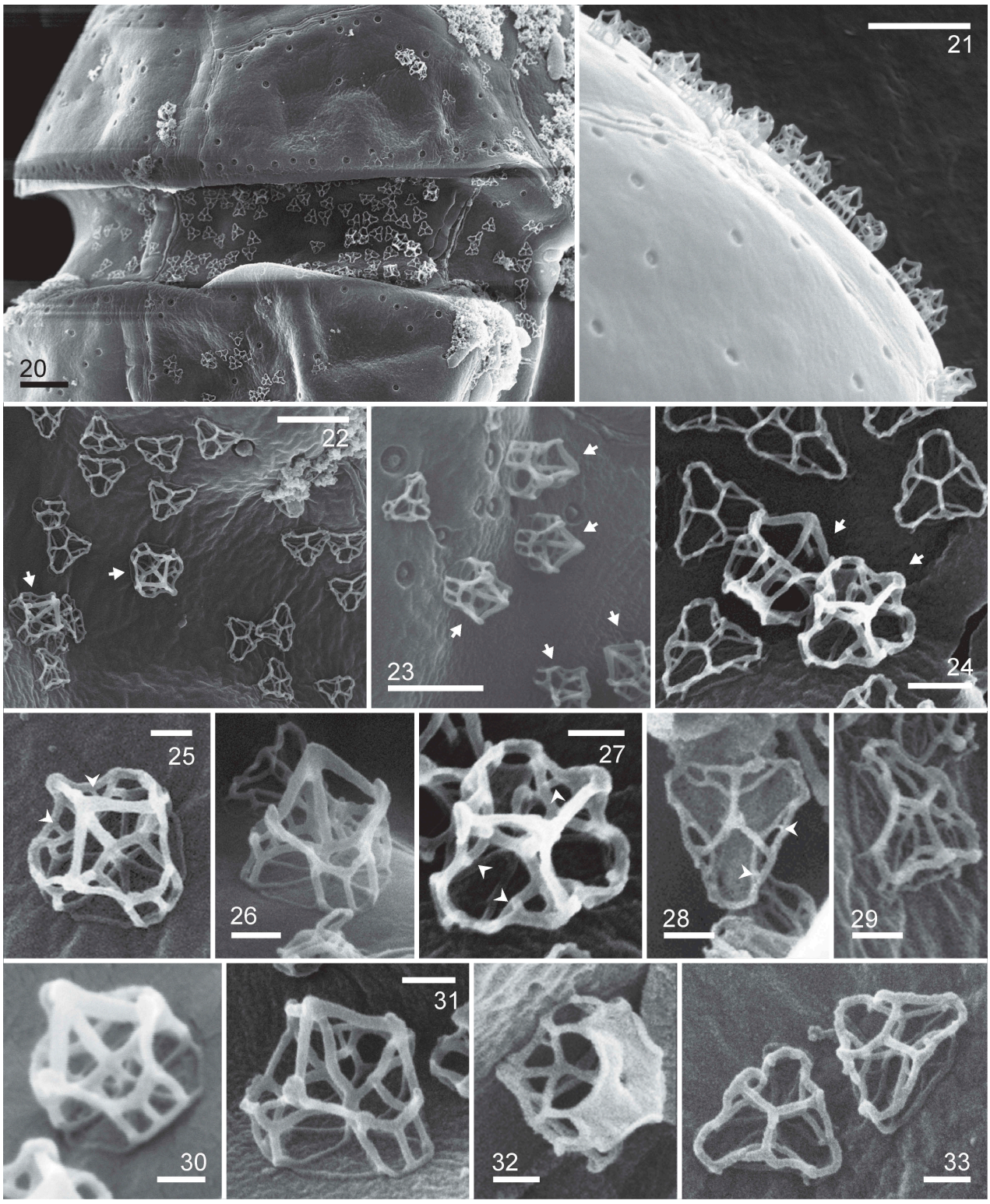

Figs 20–33. *Heterocapsa claromecoensis* sp. nov. SEM. Figs 20, 22, 24–29, 31–33. Strain LPCc-005. Figs 21, 23, 30. Strain Arg-B5. **Fig. 20**. Note trichocyst pores, denser on the marginal region of the plates, and two types of body scales on the cell surface. **Fig. 21**. Detail of the higher body scales. **Figs 22–24**. Body scales on the cell surface. Note two types of body scales, high and sub-triangular almost rounded in outline (arrows), and flat and triangular with rounded corners in outline. **Figs 25–33**. Body scales showing details of its microarchitecture. Figs 25–27, 30–32. High scales in different positions. Figs 28, 29, 33. Flat scales in different positions. Figs 25, 27, 28. Arrowheads show the small bars. Scale bars = 1 μm (Figs 20, 21), 0.5 μm (Figs 22, 23), 0.2 μm (Fig. 24), 0.1 μm (Figs 25–33).

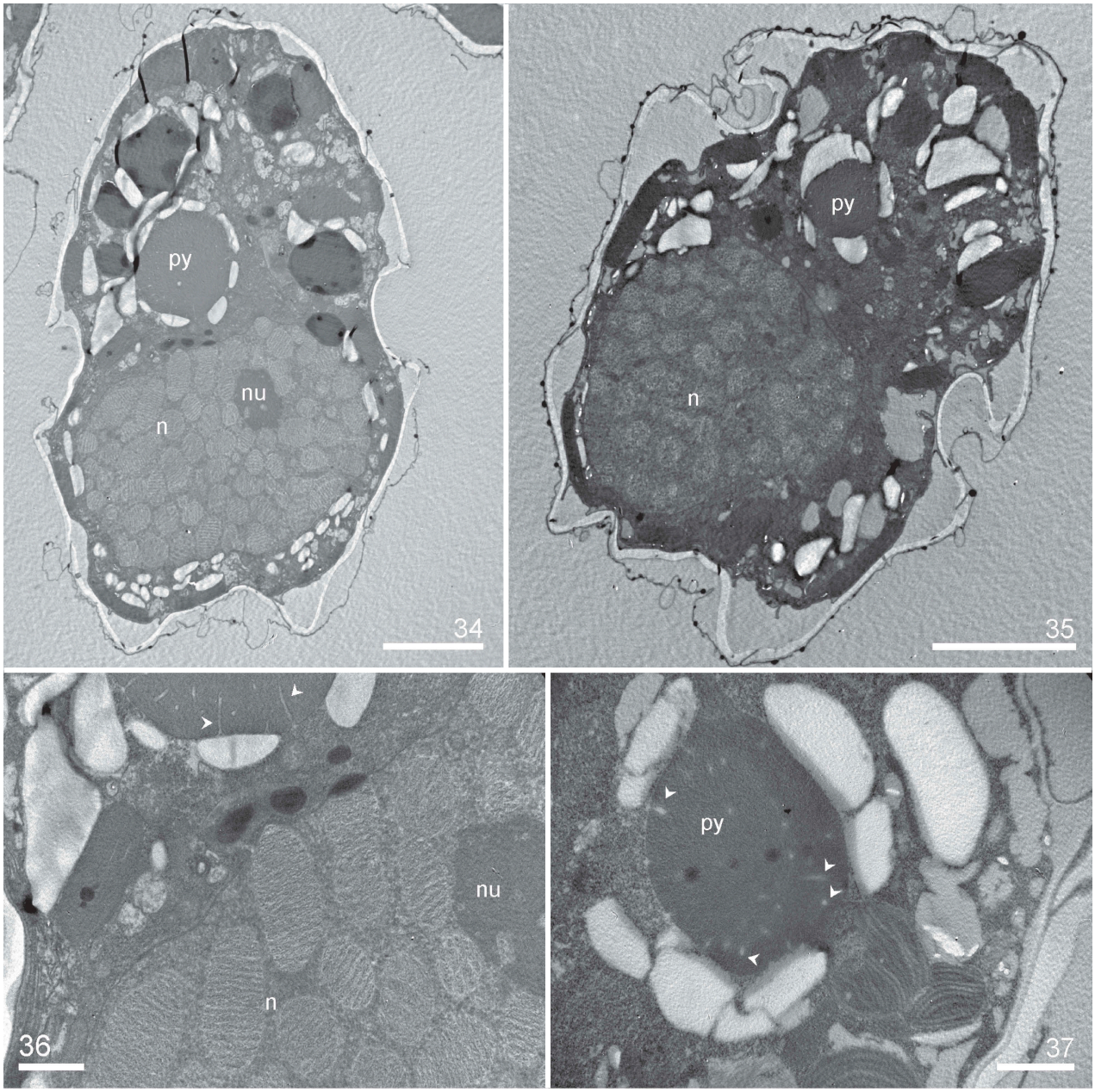

Figs 34–37. *Heterocapsa claromecoensis* sp. nov. TEM images of strain LPCc-005. **Figs 34, 35**. Longitudinal section of cells showing the large nucleus (n) and the pyrenoid (py) with starch sheath. Fig. 34. Note nucleolus (nu). **Figs 36, 37**. Details of the pyrenoid with tubular invaginations in longitudinal and transversal section (arrows). Scale bars = 5 μm (Figs 34, 35), 1 μm (Figs 36, 37).

(three transitions and one transversion). When comparing the end of the additional fragment shared exclusively between *H. orientalis* and the longer sequence of 889 nt (LPCc-005), there were additional differences (three deletions and three substitutions). Overall, *p*-distance between LPCc-005 and *H. orientalis* was 0.014. *H. niei* (Loeblich III) Morrill & Loeblich III was the second closest species, with *p*-distances between 0.079–0.086, and other related species were *H. steinii* and *H. pseudotriquetra* Iwataki, G. Hansen & Fukuyo (*p*-distances of 0.123 and 0.110–0.127, respectively). Average *p*-distances between *H. claromecoensis* and other species considered in this study were 0.087–0.177 (excluding *H. orientalis*).

For ITS, as sequences were not available for *H. orientalis*, the analysis (Fig. 49) placed *H. claromecoensis* and other sister clades on a more distant branch with *p*-distances > 0.11. *H. claromecoensis* emerged closer to the genetic groups that included *H. steinii, H. bohaiensis, H. pygmaea* Loeblich III, R.J.

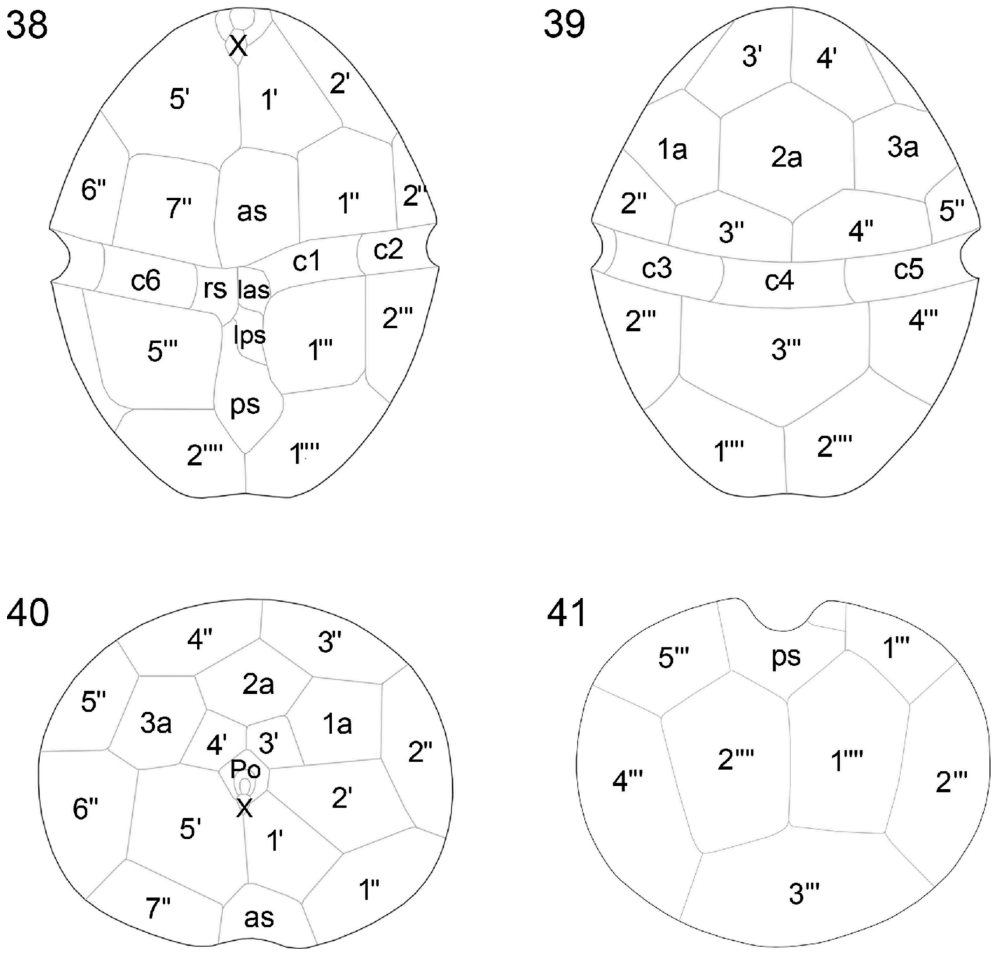

Figs 38–41. *Heterocapsa claromecoensis* sp. nov. Diagrams showing the thecal plate arrangement. **Fig. 38**. Ventral view. **Fig. 39**. Dorsal view. **Fig. 40**. Apical view. **Fig. 41**. Antapical view.

Schmidt & Sherley, *H.* cf. *pygmaea* and *H. niei*. The *p*-distance for the complete ITS rDNA region was 0.111 between *H. claromecoensis* LPCc-005 and its closest relative, *H. steinii* UTKG7, whereas for the other mentioned species *p*-distances ranged between 0.111–0.128.

Discussion

Morphological comparison

Species of *Heterocapsa* are difficult to identify using light microscopy, but the position of pyrenoid/s in relation to the nucleus is a useful character for distinguishing at least groups of species (Iwataki, 2008). *Heterocapsa claromecoensis* sp. nov. has only one pyrenoid in the episome above the nucleus which is placed in the hyposome, and is thus similar in cell organization to *H. minima* Pomroy, *H. niei, H. orientalis* and *H. psammophila* Tamura, Iwataki & Horiguchi (Table 1).

Additionally, cell size and shape can be used to aid in species identification (Iwataki, 2008). Cell size of *H. claromecoensis* is larger than cell size of *H. minima* (Salas *et al.*, 2014) and *H. psammophila* (Tamura *et al.*, 2005) (Table 1). However, cell size cannot be used to distinguish *H. claromecoensis* from *H. niei* (Loeblich III, 1968 as *Cachonina niei*) and *H. orientalis* (Iwataki *et al.*, 2003), because ranges of length and width of these species partially or almost completely overlap (Table 1).

The pattern of thecal plates for most *Heterocapsa* species is almost identical and thus of limited taxonomic value. Given the overall similarity of most *Heterocapsa* species in terms of plate pattern, the detailed body scale morphology is the ultimate ultrastructural character for distinguishing *Heterocapsa* species, except in the cases of *H. steinii* and *H. pseudotriquetra*, which have indistinguishable scales (Iwataki *et al.*, 2004). Intraspecific variation in scale structure was clearly documented by Iwataki (2004, figs 19–21, figs 22–24) for *H. arctica* Horiguchi and *H. circularisquama*, and by Rintala *et al.* (2010, fig. 3k) for *Heterocapsa arctica* var. *frigida* Rintala & G. Hällfors. Nevertheless, in all

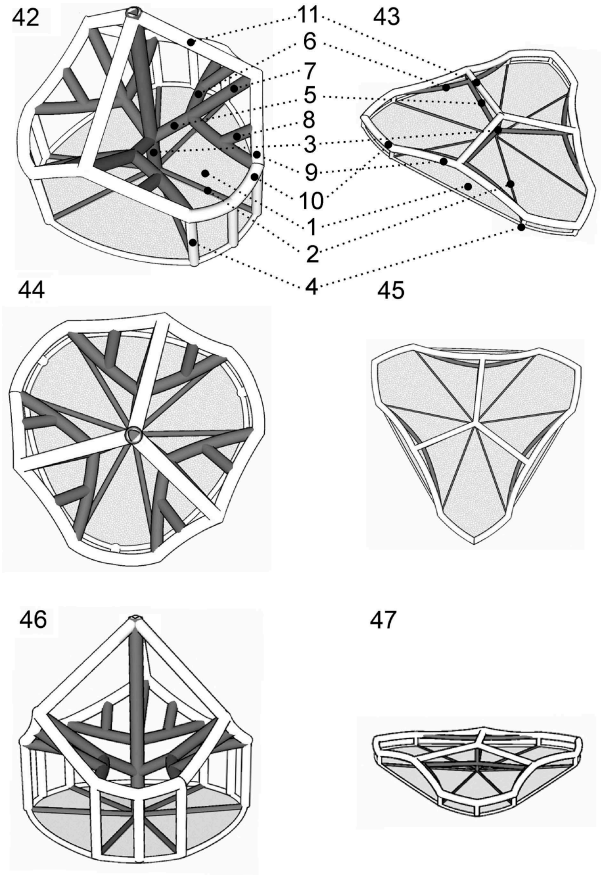

Figs 42–47. *Heterocapsa claromecoensis* sp. nov. Diagrams showing the 3-D structure of the high and flat body scales. **Figs 42, 44, 46**. High scale in different positions. **Figs 43, 45, 47**. Flat scale in the same positions as corresponding high scale. **Figs 42, 43**. Scales in lateral position showing details of their structure: 1. basal plate; 2. radial ridges (six); 3. central spine (one); 4. peripheral uprights (nine); 5. intermediate bars (three), which each furcate into two lateral bars (6) and one central bar (7); 8. small bar joining each lateral bar (6) with the corresponding longer peripheral bar (9) (six); 10. shorter peripheral bars (six); 11. upper bars (three).

these documented cases of intraspecific scale variability, all scales have the same sizes but differ in the presence or absence of horizontal bars that interconnect the peripheral uprights, and in the complexity of the 3-D construction. *Heterocapsa claromecoensis* is thus unique in having two differently sized body scales, i.e. flat, triangular with rounded corners and slightly smaller in diameter; and high scales, sub-triangular and almost rounded and slightly larger in diameter. However, despite the significant differences in height (Figs 20–33, Table 1), the microarchitecture of both types of scales is similar. Basal plates of both types have six ridges and the 3-D construction only differs in the length of the central spine and the peripheral uprights, the angle between the central spine and the upper bars, and the diameter of bars and uprights. In *H. niei* and *H. orientalis* the body scales are triangular with rounded angles, ~300 nm in diameter (Iwataki *et al.*, 2004, table 3). Scales of *H. niei* (Iwataki *et al.*, 2004, figs 33–36, 52i) differ from *H. claromecoensis* in having three radial ridges on the basal plate (vs. six), three subcentral uprights on the surface of the basal plate (vs. none), and 15 peripheral uprights (vs. 12). Scales of *H. orientalis* (Iwataki *et al.*, 2003: figs 28e, 41, 42) are similar to high scales of *H. claromecoensis* (Figs 22–27, 30–32). It has to be kept in mind that scales of *H. orientalis* were analysed with TEM (Iwataki *et al.*, 2003) and scales of *H. claromecoensis* were analysed with SEM (this study). Nevertheless, the careful 3-D reconstruction provided by Iwataki *et al.* (2003) allows a detailed comparison of scale ultrastructure. In both species, scales lack a central hole, have six radial ridges on the basal plate, one central spine, nine peripheral uprights, three intermediate bars and six shorter peripheral bars, all of similar thickness. Scales of *H. orientalis* differ from those of *H. claromecoensis* in the thickness of the elements connecting the central spine and the shorter peripheral bars with the central bars, which are thin threads in the former (Iwataki *et al.*, 2003, figs 28e, 37–42) and thick bars in the latter (Figs 24–27, 30–32, 42 ‘9’ and ‘11’). Additionally, the scales of *H. claromecoensis* but not of *H. orientalis* have small bars (Figs 25, 27, 28, 42 ‘8’), parallel to the central bars (Fig. 42 ‘7’), that connect the lateral bars (Fig. 42 ‘6’) with the corresponding longer peripheral bars (Fig. 42 ‘9’), while the scales of *H. orientalis* but not of *H. claromecoensis* present perpendicular thin threads that connect the central bars with the longer peripheral bars (Iwataki *et al.*, 2003, figs 28e, 41).

Molecular genetic analyses

Linking and/or supporting the morphological comparison and diagnosis of *H. claromecoensis* with molecular data is complicated by the fact that only partial information is available for a number of similar species. Phylogenetic analysis is additionally complicated due to a high level of mismatch between ITS barcoding placement and the corresponding *Heterocapsa* species names registered in GenBank (Stern *et al.*, 2012). Among the species with nucleus/pyrenoid position similar to *H. claromecoensis*, both LSU and ITS rDNA sequences are only available for *H. minima* and *H. niei*. Regarding *H. psammophila*, the only

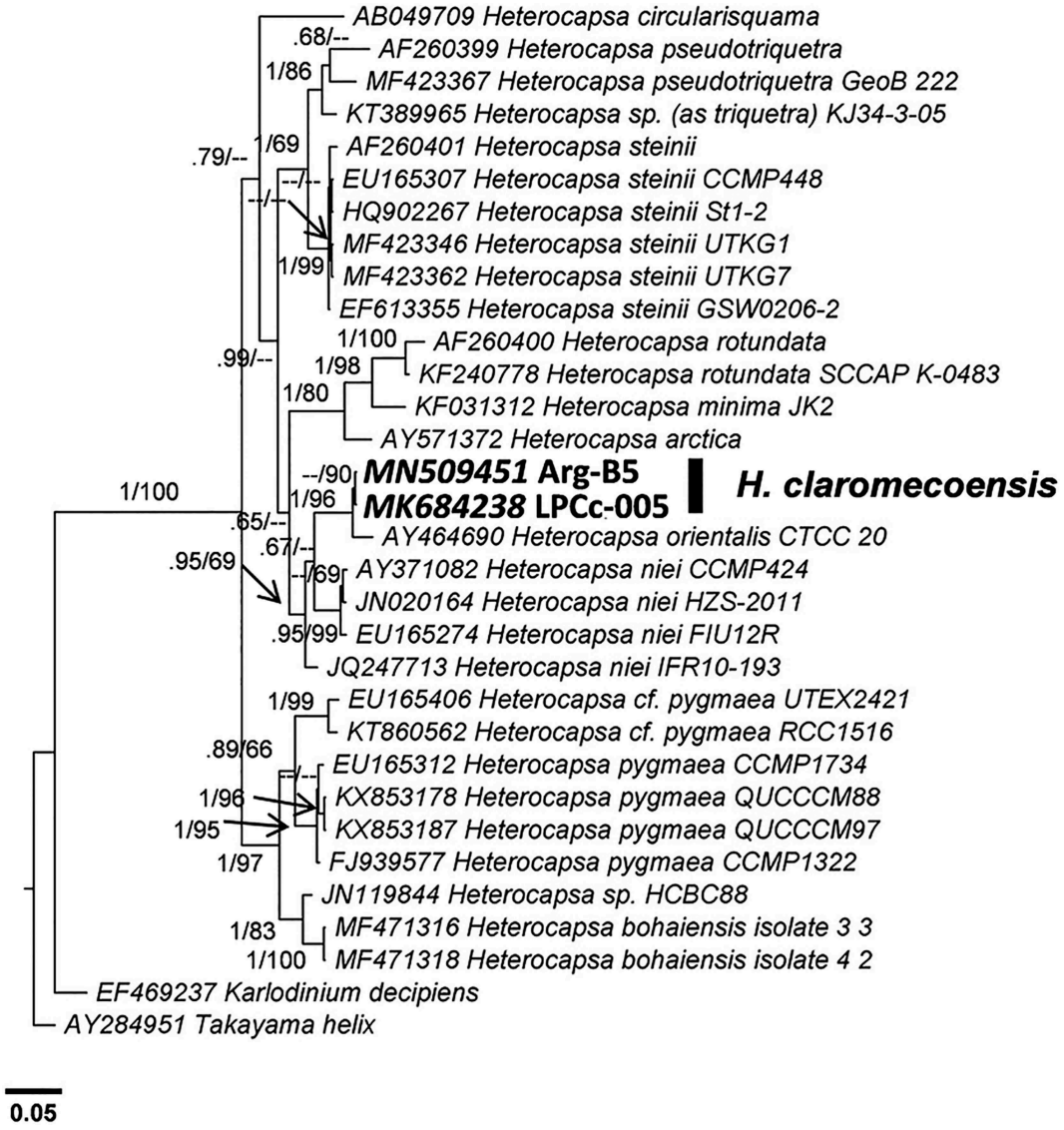

Fig. 48. Phylogenetic tree of the D1–D3 LSU rDNA showing the relationships between *Heterocapsa claromecoensis* (in bold) and other *Heterocapsa* species. Internal node supports are posterior probabilities (Bayesian analyses) and bootstrap values (Maximum likelihood). Hyphens indicate posterior probabilities < 0.6 and/or bootstrap values < 60.

sequence in GenBank is for the SSU rDNA gene, which was not sequenced in *H. claromecoensis*.

ITS data provide the largest coverage for *Heterocapsa* species, probably because the higher divergence rates allow better discrimination between closely related species (Daugbjerg *et al.*, 2000; Yoshida *et al.*, 2003; Stern *et al.*, 2012; Salas *et al.*, 2014). In terms of ITS sequences (Fig. 49), *H. claromecoensis* was distinct from all other taxa in the phylogenetic analysis. The corresponding *p*-distance values (> 0.11 from other species) are much larger than the lowest *p*-distances previously reported between species of *Heterocapsa* (0.085, Litaker *et al.*, 2007; 0.062, Xiao *et al.*, 2018). However, ITS comparison of *H. claromecoensis* is of limited value given the lack of sequence availability for some relevant species. For the morphologically most similar species, *H. orientalis*, only one partial LSU rDNA sequence with limited overlap of *H. claromecoensis* LSU is available. This sequence refers to strain CTCC20 isolated from South Africa, for which it is not clear if its morphology corresponds to the *H. orientalis* type material originating from the Iwate Prefecture, Japan (Iwataki, 2002). Consequently, corresponding low *p*-distance calculations based on LSU data (i.e. $p = 0.014$ between *H. claromecoensis* strain LPCc-005 and *H. orientalis* strain CTCC20) are of limited significance for evaluating distinctiveness (or not) between *H. claromecoensis* and *H. orientalis*. For comparison, a number of other *Heterocapsa* species,

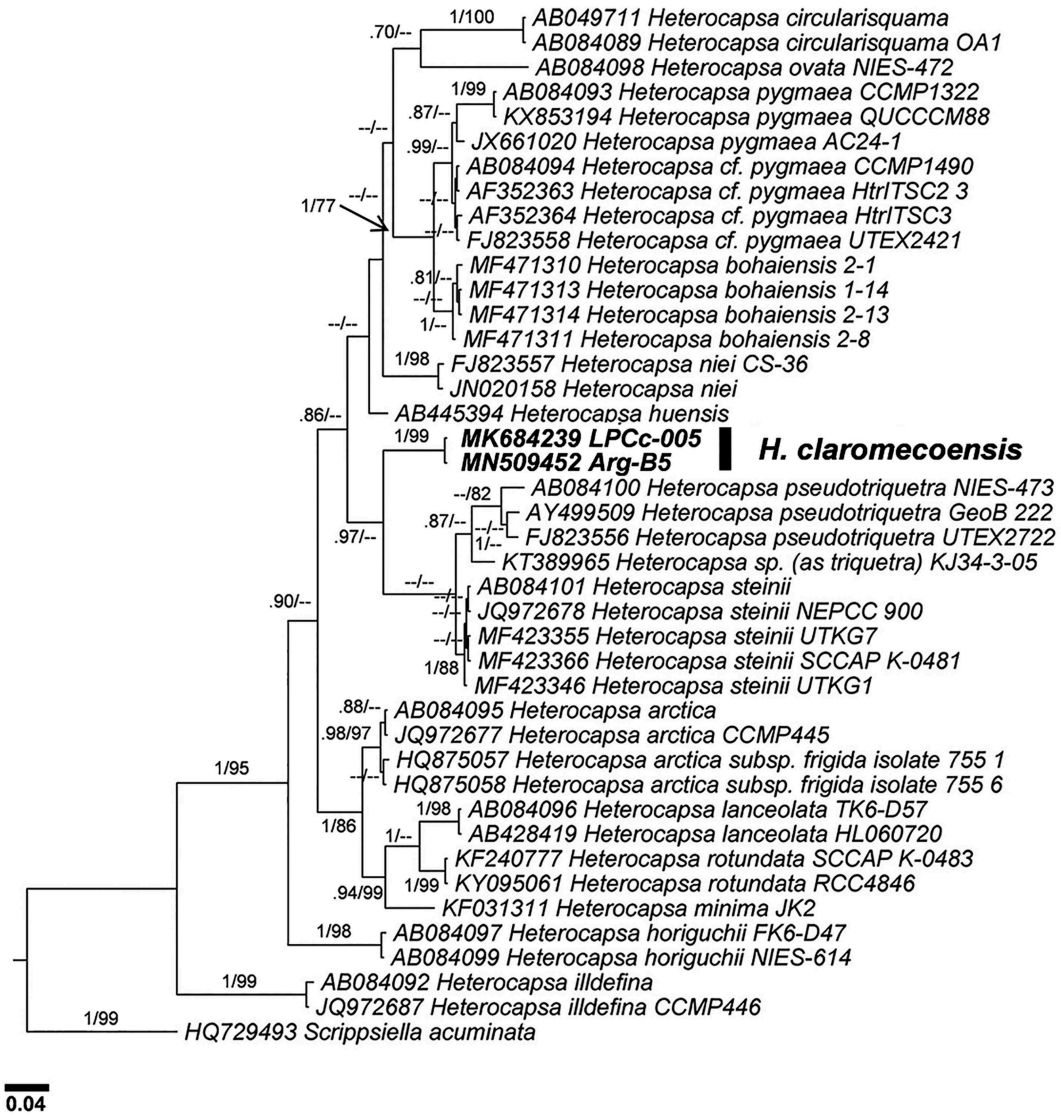

Fig. 49. Phylogenetic tree of the ITS rDNA showing the relationships between *Heterocapsa claromecoensis* (in bold) and other *Heterocapsa* species. Internal node supports are posterior probabilities (Bayesian analyses) and bootstrap values (Maximum likelihood). Hyphens indicate posterior probabilities < 0.6 and/or bootstrap values < 60.

e.g. *H. niei* and *H. pseudotriquetra*, display comparable LSU *p*-distances (> 0.013) between strains assigned to these species. In any case, even if the available molecular information does not allow confirmation that *H. claromecoensis* and strain CTCC20 are different species, *H. claromecoensis* fundamentally differs in scale morphology from the type material of *H. orientalis* described in Iwataki *et al.* (2003), supporting the erection of *H. claromecoensis* as a new species.

Acknowledgements

We thank the two anonymous reviewers for their careful analysis of the manuscript and the valuable suggestions to improve it.

Disclosure statement

No potential conflict of interest was reported by the authors.

Funding

This study was partially supported by grants from the Universidad Nacional de La Plata (11/N863), by the projects CCVIEO and DIANAS (CTM2017-86066-R) from the Instituto Español de Oceanografía and by the Alfred Wegener Institute Helmholtz Centre for Polar and Marine Research under the PACES Research Program as part of the Helmholtz foundation initiative in Earth and Environment.

Author contributions

I. Sunesen: isolation of strains, electron microscopy, morphological analyses, manuscript concept, drafting and

Table 1. Comparison between *Heterocapsa claromecoensis sp. nov.* and species with a similar nucleus/pyrenoid position.

	H. claromecoensis	*H. minima*	*H. niei*	*H. orientalis*	*H. psammophila*
References	This study	Pomroy (1989), Salas *et al.* (2014)	Loeblich III (1968), Morrill & Loeblich III (1981)	Iwataki *et al.* (2003)	Tamura *et al.* (2005)
Length in µm	16.0–30.0	10.0 –13.0	17.0–20.0	18.4–34.4	9.0–12.0
Width in µm	12.0–25.0	6.9–9.1	11.0–12.0	16.0–24.0	6.0–9.0
Cell shape	ovoidal, epitheca conical, equal in size or smaller than rounded hypotheca	ovoidal, epitheca conical, larger than rounded hypotheca	ovoidal, epitheca slightly conical, equal in size as the rounded hypotheca	ovoidal, epitheca and hypotheca hemispherical, similar in size	ovoidal, epitheca bell shaped, similar in size than bowl shaped hypotheca
Nucleus	ellipsoidal, located in the hyposome	variable in shape ranging from oval to ellipsoidal, centrally located	ellipsoidal, located in the hyposome	ellipsoidal, located in the hyposome	ellipsoidal, located in the hyposome
Pyrenoid	located in the episome, with tubular invaginations	located in the episome on its left side, ultrastructure unknown	located in the episome, without tubular invaginations	located in the episome, with many tubular invaginations	located in the episome, with tubular invaginations
Body scales (Iwataki *et al.* 2004)	250–420 nm in diameter	400 nm in diameter	300 nm in diameter	300 nm in diameter	230 nm in diameter
Basal plate	sub-triangular almost rounded and triangular with rounded poles	sub-circular	sub-triangular	sub-triangular	sub-triangular, each corner rounded with a depression
Radial ridges	6	3, bifurcated	3	6	6
Central hole	0	present	0	0	present
Central spine	< 100 nm height in flat scales; > 200 nm height in high scales	height not determined	height not determined	height not determined	height not determined
Subcentral spines on the basal plate	0	0	3	0	0
Peripheral uprights	9	6	15	9	9
Intermediate bars	3	0	0	3	3
Peripheral bars	12	6	18	12	12
Upper bars	3, similar in diameter to the central spine	0	0	3, more slender than the central spine	0
Thin threads	absent	absent	present	present	absent
Habitat	marine, phytoplanktonic	marine, phytoplanktonic	marine, phytoplanktonic forming blooms	marine, phytoplanktonic	marine, sand-dwelling

Scale morphology was interpreted from the respective references, following the terminology proposed by Iwataki *et al.* (2004) and Salas *et al.* (2014).

editing; F. Rodríguez Hernández: molecular analyses, manuscript concept, drafting and editing; J.A. Tardivo Kubis: sampling and maintaining cultures, light microscopy, DNA extraction and sequencing strain LPCc-005; D. Aguiar Juárez: light microscopy, thecal plate pattern and body scales, schemes and videos; A. Risso: maintaining cultures, microscopic identifications and counting; A.S. Lavigne: sampling, microscopic identifications and counting; S. Wietkamp: DNA extraction and sequencing strain Arg-B5; U. Tillmann: isolation of strains, electron microscopy, drafting and editing manuscript; E.A. Sar: morphological analyses, drafting and editing of manuscript and coordinating revisions.

ORCID

Inés Sunesen http://orcid.org/0000-0003-3219-456X
Francisco Rodríguez http://orcid.org/0000-0002-6918-4771
Stephan Wietkamp http://orcid.org/0000-0001-7516-9861
Urban Tillmann http://orcid.org/0000-0002-8207-4382
Eugenia A. Sar http://orcid.org/0000-0003-2912-4528

References

Arbeláez, M.N., Mancera Pineda, J.E. & Reguera, B. (2017). Dinoflagelados epífitos de *Thalassia testudinum* en dos sistemas costeros del Caribe colombiano. *Boletín de Investigaciones Marinas y Costeras*, **46**: 9–40.

Balech, E. (1988). Los dinoflagelados del Atlántico Sudoccidental. *Publicación Especial del Instituto Español de Oceanografía*, **1**: 1–310.

Daugbjerg, N., Hansen, G., Larsen, J. & Moestrup, Ø. (2000). Phylogeny of some of the major genera of dinoflagellates based on ultrastructure and partial LSU rDNA sequence data, including the erection of three new genera of unarmoured dinoflagellates. *Phycologia*, **39**: 302–317.

Fritz, L. & Triemer, R.E. (1985). A rapid simple technique utilizing Calcofluor White M2R for the visualization of dinoflagellate thecal plates. *Journal of Phycology*, **21**: 662–664.

Gottschling, M., Tillmann, U., Kusber, W.-H., Hoppenrath, M. & Elbrächter, M. (2018a). A Gordian knot: nomenclature and taxonomy of *Heterocapsa triquetra* (Peridiniales: Heterocapsaceae). *Taxon*, **67**: 179–185.

Gottschling, M., Tillmann, U., Kusber, W.-H., Hoppenrath, M. & Elbrächter, M. (2018b). (2607) Proposal to conserve the name *Heterocapsa* (Dinophyceae) with a conserved type. *Taxon*, **67**: 632–633.

Gottschling, M., Tillmann, U., Elbrächter, M., Kusber, W.-H. & Hoppenrath, M. (2019). *Glenodinium triquetrum* Ehrenberg is a species not of *Heterocapsa* F. Stein but of *Kryptoperidinium* Er.Lindem (Kryptoperidiniaceae, Peridiniales). *Phytotaxa*, **391**: 155–158.

Horiguchi, T. (1995). *Heterocapsa circularisquama* sp. nov. (Peridiniales, Dinophyceae): a new marine dinoflagellate causing mass mortality of bivalves in Japan. *Phycological Research*, **43**: 129–136.

Huelsenbeck, J.P. & Ronquist, F. (2001). MRBayes: Bayesian inference of phylogenetic trees. *Bioinformatics*, **17**: 754–755.

Iwataki, M. (2002). Taxonomic study on the genus *Heterocapsa* (Peridiniales, Dinophyceae). Department of Aquatic Bioscience, University of Tokyo, Tokyo. 144 pp.

Iwataki, M. (2008). Taxonomy and identification of the armored dinoflagellate genus *Heterocapsa* (Peridiniales, Dinophyceae). *Plankton and Benthos Research*, **3**: 135–142.

Iwataki, M., Takayama, H., Matsuoka, K. & Fukuyo, Y. (2002a). *Heterocapsa lanceolata* sp. nov. and *Heterocapsa horiguchii* sp. nov. (Peridiniales, Dinophyceae), two new marine dinoflagellates from coastal Japan. *Phycologia*, **41**: 470–479.

Iwataki, M., Takayama, H, Matsuoka, K, Hiroishi, S. & Fukuyo, Y. (2002b). Taxonomic study on *Heterocapsa* with special reference to their body scale structure. *Fisheries Science*, **68** (supplement): 631–632.

Iwataki, M., Botes, L., Sawaguchi, T., Sekiguchi, T. & Fukuyo, Y. (2003). Cellular and body scale structure of *Heterocapsa ovata* sp. nov. and *Heterocapsa orientalis* sp. nov. (Peridiniales, Dinophyceae). *Phycologia*, **42**: 629–637.

Iwataki, M., Hansen, G., Sawaguchi, T., Hiroishi, S. & Fukuyo, Y. (2004). Investigations of body scales in twelve *Heterocapsa* species (Peridiniales, Dinophyceae), including a new species *H. pseudotriquetra* sp. nov. *Phycologia*, **43**: 394–403.

Iwataki, M., Kawami, H., Van Nguyen, N., Luong, Q.D., Ton, T.P., Fukuyo, Y. & Matsuoka, K. (2009). Cellular and body scale morphology of *Heterocapsa huensis* sp. nov. (Peridiniales, Dinophyceae) found in Hue, Vietnam. *Phycological Research*, **57**: 87–93.

Keller, M.D., Selvin, R.C., Claus, W. & Guillard, R.R.L. (1987). Media for the culture of oceanic ultraphytoplankton. *Journal of Phycology*, **23**: 633–638.

Ki, J.S. & Han, M.S. (2007). Informative characteristics of 12 divergent domains in complete large subunit rDNA sequences from the harmful dinoflagellate genus, *Alexandrium* (Dinophyceae). *Journal of Eukaryotic Microbiology*, **S4**: 210–219.

Kotob, S.I., McLaughlin, S.M., Van Berkum, P. & Faisal, M. (1999). Discrimination between two *Perkinsus* spp. isolated from the softshell clam, *Mya arenaria*, by sequence analysis of two internal transcribed spacer regions and the 5.8S ribosomal RNA gene. *Parasitology*, **199**: 363–368.

Kumar, S., Stecher, G. & Tamura, K. (2016). MEGA7: Molecular Evolutionary Genetics Analysis Version 7.0 for bigger datasets. *Molecular Biology and Evolution*, **33**: 1870–1874.

Lenaers, G., Maroteaux, L., Michot, B. & Herzog, M. (1989). Dinoflagellates in evolution: a molecular phylogenetic analysis of large subunit ribosomal RNA. *Journal of Molecular Evolution*, **29**: 40–51.

Lindemann, E. (1924). Der Bau der Hülle bei *Heterocapsa* und *Kryptoperidinium foliaceum* (Stein) n. nom. (Zugleich eine vorläufige Mitteilung). *Botanisches Archiv*, **5**: 114–120.

Litaker, R.W., Vandersea, M.W., Kibler, S.R., Reece, K.S., Stokes, N.A., Steidinger, K.A., Millie, D.F., Bendis, B.J., Pigg, R.J. & Tester, P.A. (2003). Identification of *Pfiesteria piscicida* (Dinophyceae) and *Pfiesteria*-like organisms using internal transcribed spacer-specific PCR assays. *Journal of Phycology*, **39**: 754–761.

Litaker, R.W., Vandersea, M.W., Kibler, S.R., Reece, K.S., Stokes, N.A., Lutzoni, F.M., Yonish, B.A., West, M.A., Black, M.N.D. & Tester, P.A. (2007). Recognizing dinoflagellate species using ITS rDNA sequences. *Journal of Phycology*, **43**: 344–355.

Loeblich III., A.R. (1968). A new marine dinoflagellate genus *Cachonina* in axenic culture from the Salton Sea, California, with remarks on the genus *Peridinium*. *Proceedings of the Biological Society of Washington*, **81**: 91–96.

Morrill, L.C. & Loeblich III, A.R. (1981). A survey for body scales in dinoflagellates and a revision of *Cachonina* and *Heterocapsa* (Pyrrhophyta). *Journal of Plankton Research*, **3**: 53–65.

Nei, M. & Kumar, S. (2000). *Molecular Evolution and Phylogenetics*. Oxford University Press, New York.

Pomroy, A.J. (1989). Scanning electron microscopy of *Heterocapsa minima* sp. nov. (Dinophyceae) and its seasonal distribution in the Celtic Sea. *British Phycological Journal*, **24**: 131–135.

Richlen, M.L. & Barber, P.H. (2005). A technique for the rapid extraction of microalgal DNA from single live and preserved cells. *Molecular Ecology Notes*, **5**: 688–691.

Rintala, J.M., Hällfors, H., Hällfors, S., Hällfors, G., Majaneva, M. & Blomster, J. (2010). *Heterocapsa arctica* subsp. *frigida* subsp. nov. (Peridiniales, Dinophyceae). Description of a new dinoflagellate and its occurrence in the Baltic Sea. *Journal of Phycology*, **46**: 751–762.

Rodríguez, F., Fraga, S., Ramilo, I., Rial, P., Figueroa, R.I., Riobó, P. & Bravo, I. (2017). Canary Islands (NE Atlantic) as a biodiversity 'hotspot' of *Gambierdiscus*: implications for future trends of ciguatera in the area. *Harmful Algae*, **67**: 131–143.

Salas, R., Tillmann, U. & Kavangh, S. (2014). Morphological and molecular characterization of the small armoured dinoflagellate *Heterocapsa minima* (Peridiniales, Dinophyceae). *European Journal of Phycology*, **49**: 413–428.

Stein, F. (1883). *Der Organismus der Infusionsthiere nach eigenen Forschungen in systematischer Reihenfolge bearbeitet. III. Abtheilung. II. Hälfte. Die Naturgeschichte der Arthrodelen Flagellaten*. W. Engelmann, Leipzig. 30 pp.

Stern, R.F., Andersen, R.A., Jameson, I., Küpper, F.C., Coffroth, M.-A., Vaulot, D., Le Gall, F., Véron, B., Brand, J.J., Skelton, H., Kasai, F., Lilly, E.L. & Keeling, P.J. (2012). Evaluating the ribosomal internal transcribed spacer (ITS) as a candidate dinoflagellate barcode marker. *PLoS ONE*, **7**(8): e42780.

Tamura, M., Iwataki, M. & Horiguchi, T. (2005). *Heterocapsa psammophila* sp. nov. (Peridiniales, Dinophyceae), a new sand dwelling marine dinoflagellate. *Phycological Research*, **53**: 303–311.

Tillmann, U., Hoppenrath, M., Gottschling, M., Kusber, W.-H. & Elbrächter, M. (2017a). Plate pattern clarification of the marine dinophyte *Heterocapsa triquetra* sensu Stein (Dinophyceae) collected at the Kiel Fjord (Germany). *Journal of Phycology*, **53**: 1305–1324.

Tillmann, U., Jaén, D., Fernández, L., Gottschling, M., Witt, M., Blanco, J. & Krock, B. (2017b). *Amphidoma languida* (Amphidomataceae, Dinophyceae) with a novel azaspiracid toxin profile identified as the cause of molluscan contamination at Atlantic coast of southern Spain. *Harmful Algae*, **62**: 113–126.

Tillmann, U., Hoppenrath, M. & Gottschling, M. (2019). Reliable determination of *Prorocentrum micans* Ehrenb. (Prorocentrales, Dinophyceae) based on newly collected material from the type locality. *European Journal of Phycology*, **54**: 417–431.

Turland, N.J., Wiersema, J.H., Barrie, F.R., Greuter, W., Hawksworth, D.L., Herendeen, P.S., Knapp, S., Kusber, W.-H., Li, D.-Z., Marhold, K., May, T.W., McNeill, J., Monro, A.M., Prado, J., Price, M.J. & Smith, G.F. (eds) (2018). *International Code of Nomenclature for Algae, Fungi, and Plants (Shenzhen Code) Adopted by the Nineteenth International Botanical Congress, Shenzhen, China, July 2017*. Regnum Vegetabile 159. Koeltz Botanical Books, Glashütten. https://doi.org/10.12705/Code.2018.

Xiao, J., Sun, N., Zhang, Y., Sun, P., Li, Y., Pang, M. & sLi, R. (2018). *Heterocapsa bohaiensis* sp. nov. (Peridiniales: Dinophyceae): a novel marine dinoflagellate from the Liaodong Bay of Bohai Sea, China. *Acta Oceanologica Sinica*, **37**: 18–27.

Yoshida, T., Nakai, R., Seto, H., Wang, M-K., Iwataki, M. & Hiroshi, S. (2003). Sequence analysis of 5.8S rDNA and the Internal Transcribed Spacer region in dinoflagellate *Heterocapsa* species (Dinophyceae) and development of selective PCR primers for the bivalve killer *Heterocapsa circularisquama*. *Microbes and Environments*, **18**: 216–222.